

Numerical Simulation of the Stress, Temperature & Wear Behaviours of the Drum Brake

Ehtisham Shahid¹, Xiaoying Wang¹, Zijie Fan¹, Liangjin Gui^{1*}

¹State Key Laboratory of Automotive Safety and Energy, Department of Automotive Engineering Tsinghua University, Beijing 100084, China.

*E-mail: gui@tsinghua.edu.cn

Abstract. Thermo-mechanical coupling phenomena exist in the drum brake, which produces high contact stress field and transient temperature. Kinetic and Potential energies are applied and transformed into thermal energy and that thermal energy couples the different attributes such as stress, temperature, and wear. In this paper, the Archard abrasive wear model and Finite Element Method (FEM) are combined to simulate the normal braking condition of drum brake by means of the stress and wear coupled analysis method. Then based on stress, temperature and wear coupling method, the brake is simulated under emergency braking condition by using ABAQUS. UMESHMOTION subroutine is coded to realize the material loss. The process shows the contact pressure area, temperature field and wear abruption and their coupling process. Stress, temperature and wear are associated with expansion properties of a substance which are discussed in undeviating simulation results. Keywords-Wear; Drum brake; FEM; Heat flux; FEA.

1. Introduction

Drum brake has a strong, complex and intense level of thermal stress and coupled wear while braking. Due to pressure, friction plates and drum crushes while coming into contact with each other and cause severe friction. Work done by friction produces a huge amount of heat and temperature. The friction force is the cause of heat so it directly affects the heat transfer and conduction. The sudden rise of temperature changes the stiffness of friction plates, the hardness of brake drum and the interfacial friction factors. Meanwhile, Uneven thermal deformation affects the surface of the drum in brake which brings the change in the distribution of friction and contact pressure along with the wear attribute. In turn, wear behaviour changes the contact surface's state which often affects the distribution of contact pressure. Hence, braking process is fully related to coupled stress, temperature and wear attributes [1,2].

Coupling problem of stress, temperature and wear involve complex structural geometry and nonlinear behaviours in contact so it is hard to obtain accurate analytical solutions. In the present time, many of the researchers and scholars have been using FEM to solve the thermal-stress coupling process problems in braking systems [3,4]. However, the research on thermal boundary conditions was a



breakthrough in its own and made things lot simple in the field of tribology but wear and tear factor was totally ignored on the temperature and displacement impact on the coupled surface.

At the end of last century, the research on wear began by using FEM [5,6]. Based on Adaptive Lagrangian-Eulerian (ALE) method the adaptive wear model was studied for radial bearing with the rotation process at the time of shaft contact and the bondage of wear was smaller than the surface height [7].

However, the solution is simply suitable for simple structural problems and for real life practical engineering problems but there is still a great distance to cover [8,9]. The effect of wear and influence of thermo-elastic instabilities in mechanical coupling and the seriously deviated stress results from the actual situation were studies under developed FEM methods on the bases of elastic-mechanical equation etc., just as a 2D model with Hertzian pressure distribution [10,11].

Starting with the stress and wear coupling algorithm for the simulation of the friction in a drum brake, along with that the 3D model of drum brake is developed for transient braking and temperature reduction analysis. The process includes an interaction of stress, temperature and wear depend on the thermal parameters along with the temperature of materials. The simulation results are verified in terms of stress, temperature, and wear.

2. Method and mathematical model of stress temperature and wear

2.1. Thermal-stress coupling and boundary conditions

- All materials used in the model, including brake drum and friction plates are fully isotropic, homogeneous and uniform.
- There is no source of heat inside the material because the whole deformation doesn't get into plastic deformation and no damping factor is found.
- In the whole braking process, the inertial forces are completely ignored and considered main forces are the contact force and the frictional force so that the mechanical analysis can be done including thermodynamic properties because following model's contact conditions are very strong and deformation or mesh distortion is possible.

Three Dimensional heat conduction is required to be considered in a model in which the temperature and are could be expressed with regard to spherical coordinates and cylindrical co-ordinates (Cartesian co-ordinates). Temperature field and the material's density are expressed as well along with thermal conductivity and specific heat capacity [12].

The boundary condition for convective heat transfer has to be declared along with heat convection and a decrease in temperature coefficients. The boundary condition for friction heat flux has to be declared along with the relative velocity of sliding surface or relative sliding rate [13,14].

By using FEM, deformation needs to be considered. The displacement has to be declared by following the elastic model and need a supposition for minor deformation.

$$\begin{bmatrix} 0 & 0 \\ 0 & C_{\emptyset} \end{bmatrix} \begin{Bmatrix} \dot{u} \\ \Delta\emptyset \end{Bmatrix} + \begin{bmatrix} K_u & -K_{u\emptyset} \\ 0 & K_{\emptyset} \end{bmatrix} \begin{Bmatrix} u \\ \Delta\emptyset \end{Bmatrix} = \begin{Bmatrix} fu \\ \Delta P_{q(p)} + \Delta P_H \end{Bmatrix} \quad (1)$$

In the equation above C_{\emptyset} is the matrix for the heat capacity, K_{\emptyset} is the matrix for the heat conduction or thermal conductivity, \emptyset is the vector of temperature at nodes, P is the load vector of temperature at nodes, P_q is the head-induced load vector caused by the heat generation and it is a function of contact pressure p . The load vector caused by convective heat dissipation is P_H . K_u is the displacement on the nodes for node matrix, $K_{u\emptyset}$ is the node temperature's contribution towards the nodal force matrix, u and fu both are the displacement vector and force vector of the node, respectively.

Coupled FEM involves stress and temperature. By considering equation (1) the whole drum brake can be heated all over. Heat convection equation is [15, 16].

$$q = h_c A \Delta T \quad (2)$$

In the equation above q is the heat transfer per unit time, A is the heat transfer area of the surface, h_c is the convective heat transfer coefficient of the outer surface of the brake drum and the scrounging and ΔT is the temperature difference between the brake drum and friction plates.

$$h_c = \frac{k_l Nu}{l} \quad (3)$$

Here, Nu is the Nusselt number, k_l is the thermal conductivity and l is the outer diameter of the brake drum with the characteristic length of the Reynold number.

2.2. Contact properties

The Suppose if there is a contact between two different objects taken as points are A and B then momentum equilibrium condition can be considered [17], which includes the component of normal force, and properties.

When objects come into contact then sometimes there is a penetration and sometimes not so it can be calculated by using mutual penetration rate of objects, their normal velocity, and normal contact conditions.

2.3. Wear modeling

The numerical integration of wear is based on the Euler method. The incremental form of generalized Archard wear model is [18].

$$\Delta h = kp \Delta s \quad (4)$$

In the above formation Δh is the increment for wear thickness, k is the coefficient for wear factor, Δs is the increment for relative displacement.

By assuming the contact nodes of the brake drum and the friction plates in finite element mesh is i and the integration step is j then the wear increment is as followed.

$$\Delta h(i, j) = k(i, j) p(i, j) \Delta s(i, j) \quad (5)$$

Then the cumulative wear is appeared as,

$$h(i, j) = \sum_{l=1}^j \Delta h(i, j) = \sum_{l=1}^j k(i, l) p(i, l) \Delta s(l) \quad (6)$$

3. Numerical simulation of normal and emergency braking process

In order to keep simulation results of stress and wear more accurate, it is necessary to simulate the brake's normal braking process to achieve smooth contact after executing finite element model because there are some errors left behind as uneven friction surface due to installation errors or scientific errors while manufacturing etc., which may cause poor contact while start-up if brake is not in normal braking process.

3.1. FEM model

The finite element model of the drum brake from the rear axle of heavy duty vehicle is created by using the Hypermesh software after illumination of some unnecessary components like springs, pins, cables, holders etc., 'figure 1'. The number of elements are 10466 (15841 NODES). The whole drum is simulated by using first-order element type C3D8RT because this is one of the units which can be

simulated better under complex surfaces and improve contact conditions during analysis. The both friction plates have adopted first-order element type C3D8RT as well. Meanwhile, the brake shoes containing shell element type S4RT and the rollers are replaced, because the cam forces on the brake shoes have no direct impact on the wear and tear. Instead of rollers, the analytical rigid beams connected to control points are used to receive force and to impose a corresponding constant concentration.

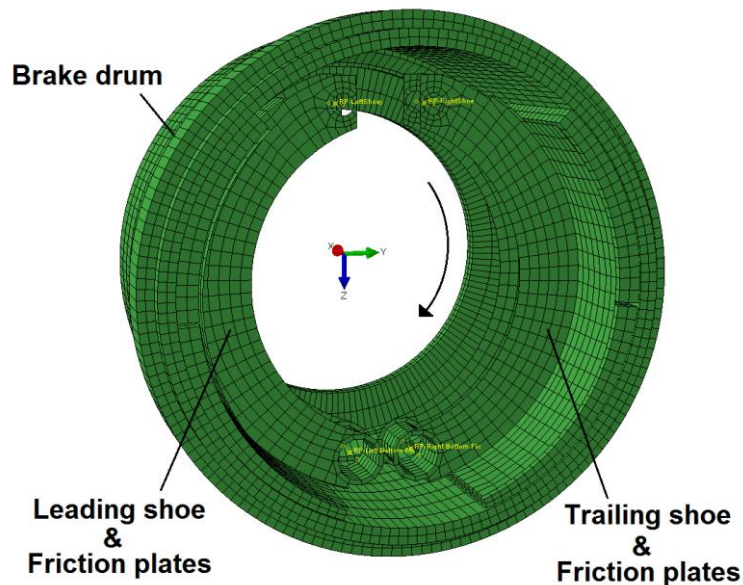


Figure 1. Finite Element Model of drum brake.

The brake drum is made up of material tagged as HT250 as per Chinese standard and regulations. Brake shoes are made up of Steel. Friction plates are made up of composite material. All the parameters and properties for brake drum, friction plates and shoes are shown in table 1.

Table 1. Material properties of drum brake.

	Temp. (°C)	Specific heat ($J/(kg \cdot ^\circ C)$)	Conductivity ($W/(m \cdot ^\circ C)$)	Thermal expansion ($10^{-6}/^\circ C$)	Young's modulus (GPa)	Density (kg/m^3)	Poisson's ratio
Drum	20	503	42.38	04.386	100.000	7220	0.3
	100	530	43.06	11.653	-	7220	0.3
	200	563	44.23	12.836	099.693	7220	0.3
	300	611	43.55	13.580	-	7220	0.3
	400	641	40.67	13.578	096.273	7220	0.3
	500	701	39.72	13.804	-	7220	0.3

Friction plates	-	1178	01.98	07.550	007.650	2150	0.3
Shoes	-	452	48.00	11.000	205.000	7800	0.3

While the wear coefficient for the friction plates is $k = 15 \times 10^{-15} Pa$. Attributes of the model include absolute zero temperature $1 \times 10^{-9} \text{ }^\circ\text{C}$ and Stefan-Boltzmann constant $5.669 \times 10^{-8} \text{ J}/\text{sm}^2\text{k}^{-4}$. The value used for heat convection and surface film condition is $50 \text{ W}/(\text{m}^\circ\text{C})$, as film coefficient depends on circumstances and varies accordingly.

The reference points (RP) are shown in the 'figure 2'. During simulation, the inner part of the cylinder is coupled to flange surface through multi-point constraint (MPC) from its surface to control point at drum's axis of rotation denoted by RP-Drum in 'figure 2a'.

In the brake shoes, the bottom end is hinged with the brake plate and during the simulation, and the nodes are coupled to the inner surface of pin holes and its contact point on the axes of nodes by using MPC denoted by RP-Left Bottom Fix and RP-Right Bottom Fix in 'figure 2b'. In an actual braking system, the upper end of shoes is connected with a roller at the top so the upper hole surface section is required and the circular nodes are coupled with the control points on their control axis point. Rollers are replaced and controlled by the rotation point on the axis denoted by RP-LeftShoe and RP-RightShoe. These two control points are linked with the control points on the axis by using beam type elements through MPC.

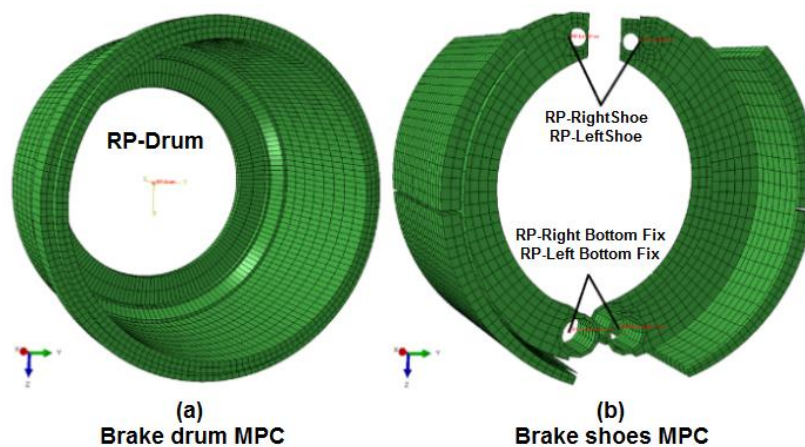


Figure 2. Reference points and multi-point constraints.

The contact between the brake drum and the friction plates is mainly defined between the inner surface of the brake drum and the outer layer of friction plates. The contacting algorithm for friction plates is the Penalty friction formulation and the friction coefficient is 0.35. The constraints between friction plates and brake shoes are tie constraints. In the normal braking process, the brake torque is about 17550.5Nm.

3.2. Solution

As it was mentioned earlier that in the whole normal braking process the inertial forces are completely ignored. Neglecting the inertial forces effect belongs in a quasi-static process (2).

The UMESHMOTION subroutine has been used to calculate the adjacent incremental steps of the stress analyzation. Then ALE is used to update the finite element mesh to realize the wear simulation by incremental stress in the incrimination step and then update the wear amount.

In the start, the displacement loads are pre-applied on the contacted surfaces so that the contact calculation of each contact pair converges properly. Then displacement loads are removed and a load is applied at RP-LeftShoe and RP-RightShoe. Then the constant rotation speed of brake drum is set at the brake drum control point denoted as RP-Drum, $\omega=26.455\text{rad/s}$. Parameters are set for normal braking simulation process.

During the simulation, the wear of the brake drum is ignored and the friction material is set as the ALE domain. Then the wear on the surface of friction plates is calculated by UMESHMOTION subroutine. Process using thermal-stress-wear coupling method is shown in the 'figure 3'. Processing method is split into parts as frictional contact process is combined with the material removed from surface and thermo-elastic distortion. On the bases of their FEM substructure, they have been solved in ABAQUS where mechanical and thermal results can be attained together. Adaptive mesh tool and the UMESHMOTION subroutine are used together in ABAQUS to adjust the position of on surface nodes according to material loss induced by wear.

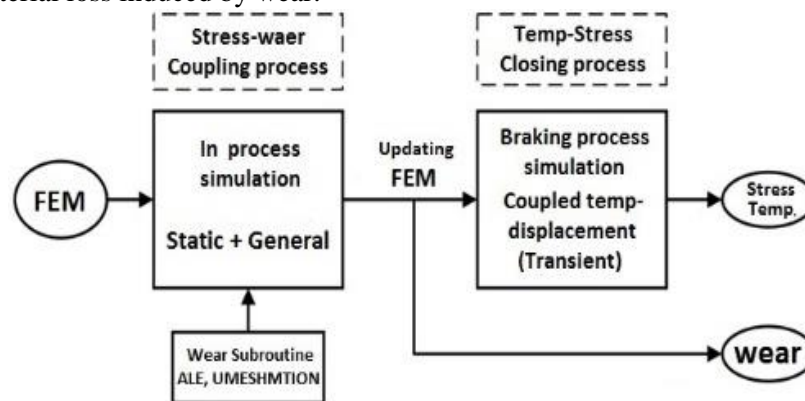


Figure 3. Thermo-mechanical & wear coupling.

3.3. Solution result and analysis

Evolution of the contact pressure of friction plates can be seen in 'figure 4'. First part represents the initial pressure distribution on leading and trailing shoe at the initial time. Second half represents the contact pressure distribution at the time of completion of the running process on leading and trailing shoe. It can be seen from the 'figure 4' that most of the friction plates area has come into contact with the inner surface of the brake drum.

At the initial moment, the contact pressure distribution is very much uneven. In the leading shoe, the contact pressure is greater than the trailing shoe due to the lifting force.

Right after the start of the running the area where the contact pressure is observed, shows that the contact is improved in the area where contact pressure is large and contact pressure increased gradually. At the end of the normal braking process, the maximum contact pressure is distributed across most of the area of friction plates. It shows that the contact pressure distribution is more uniform and graphically from most of the area it is accessible to differentiate by colours.

While in the normal braking process the contact pressure and stress distribution along the brake drum axil can't be neglected and has certain characteristics. In 'figure 4' the left side of the left friction plate is in the direction of brake drum flange. The right side of the right friction plate is in the direction of brake drum flange. The part of friction plates close to the brake drum flange has greater contact pressure than the part of friction plates at the opening of a brake drum. The flange side of brake drum has fix constraints so stiffness is relatively larger than the opening side of a brake drum.

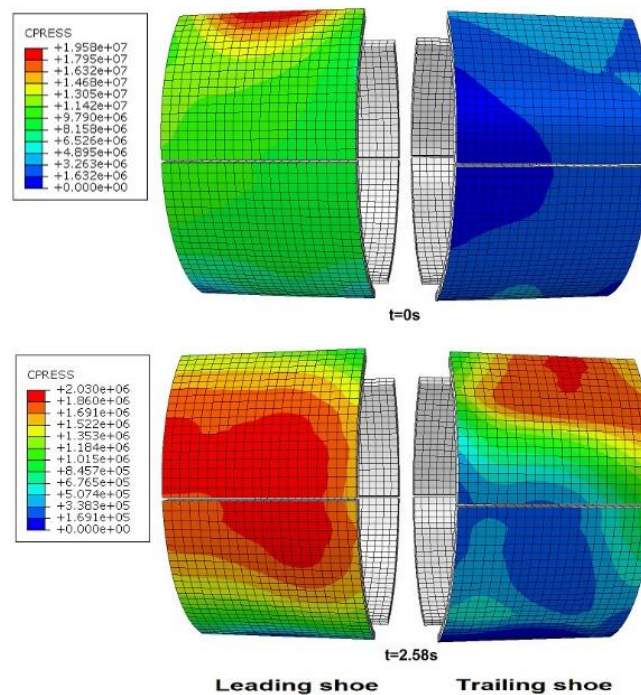


Figure 4. Contact pressure distribution in normal braking condition.

After the normal braking process, the friction plates are in the good contact form with the brake drum. Now in the emergency braking condition, the effect of temperature is considered. In the step when loads are applied the brake time is 2.58s and the rotation speed of brake drum is 26.455rad/s which constantly decelerated up to 0.

The concentrated forces added on the Left and Right friction plates are calculated by finite element software. Concentrated forces can be seen in table 2.

Table 2. Applied load on brake shoes.

	Load Point	CF1(N)	CF2(N)	CF3(N)
Leading shoe	RP-LeftShoe	000	-36037.3	12041
Trailing shoe	RP-RightShoe	000	50622.4	-18137.6

The contact and heat flux between the brake drum and friction plates are mentioned earlier in [1]. When brake drum is in contact with a friction plate, the set coefficient for heat flux is large to ensure that temperature at contact points are the same.

Distribution of contact pressure during emergency braking is shown in the 'figure 5'. In leading shoe, the contact status is improved because of the role of the entire friction plate so the distribution of contact pressure is relatively uniform and the left side of friction plate is beside flange of the brake drum, so the contact pressure is a bit more than other portions of the friction plate. Some of the visible effects can be observed in trailing shoe.

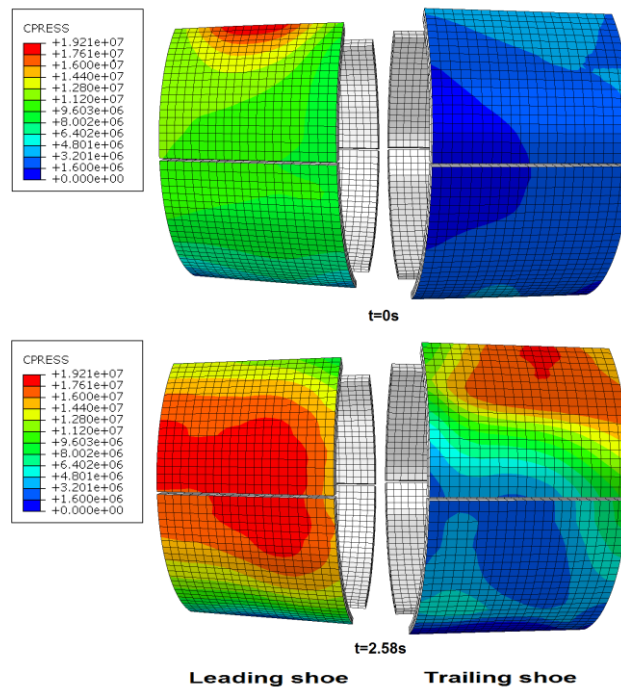


Figure 5. Contact pressure distribution in emergency braking condition.

The amount of wear of the friction plates is shown in the ‘figure 6’. The sliding surface of drum brake is nearly equal to each other in the braking process so the amount of wear and contact pressure distribution is nearly close. At the end of braking process where contact pressure was maximum, the observed intensity of wear depth has a minute value of 0.425µm.

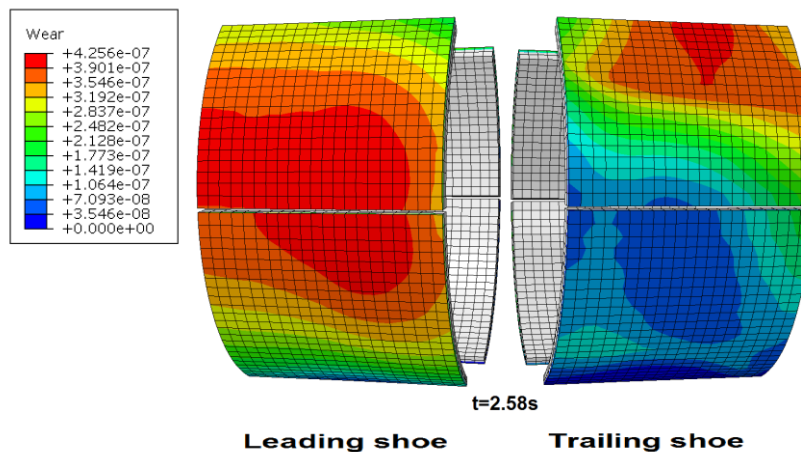


Figure 6. Wear depth - Emergency braking condition.

The changes in temperature of the brake drum and friction plates and its distribution during the whole braking process is shown in the ‘figure 7’. At an initial time when $t=0.10s$ the temperature of friction plates and brake drum is not that large but temperature distribution is so uneven.

Contact pressure and the frictional thermal flux is directly proportional to each other so because of this relation the frictional temperature of leading shoe rises higher than the frictional temperature of trailing shoe.

Along with that, the area of friction plates which are near to brake drum flange has the high frictional temperature and pressure than the other areas of friction plates on the open end of a brake drum.

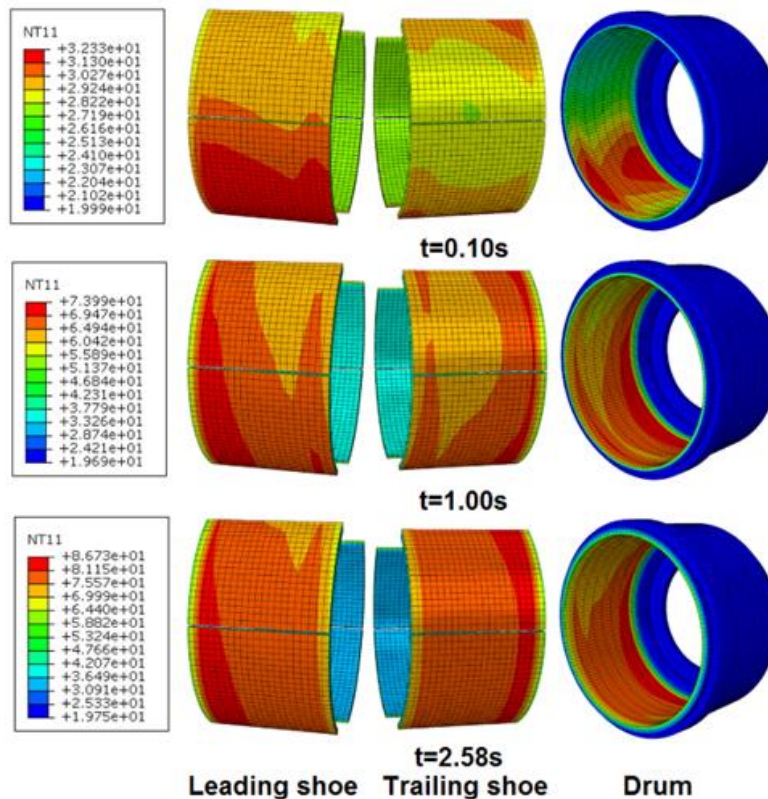


Figure 7. Temperature evaluation at different times in emergency braking condition.

The contact between friction plates and the brake drum are good enough so the temperature and pressure distributions are almost axisymmetric. Because of good contact between surfaces the inner surface of the brake drum and the outer surfaces of friction plates are not with much difference, nearly the same.

4. Conclusion

In this paper, an algorithm has been formed to consider thermo-mechanical coupling and tribological properties including stress, temperature and wear for drum brake based on FEA. The normal braking process of drum brake is numerically simulated to compare the effect and distribution of wear with contact pressure, stresses and temperature simultaneously.

- The stress-temperature-wear coupling simulation algorithm is used in normal braking process, then results along with the evaluation of the contact pressure is shown. From the results, the contact pressure can be evaluated while interacting with temperature field.
- From the whole research, the results indicate that in normal braking process the contact pressure of leading shoe is larger than the trailing shoe. The contact pressure at the both ends of the both shoes are higher than the middle area. The contact pressure of the friction plates is

greater on the sides which are near to the flange of brake drum than the sides which are on the opening end. The contact pressure distribution tends to be uniform.

- The temperature field distribution of brake drum is approximately axisymmetric. The friction plates have the lower temperature on the sides which are near to the flange and higher temperature on the sides which are on the opening end.
- Friction plates wear is far larger than the brake drum so only friction plates wear has been considered in the simulation. ALE method sets a load and friction for materials as a whole and UMESHMOTION subroutine calculates joint wear for frictional surfaces.

5. Acknowledgement

The authors would like to acknowledge the National Natural Science Foundation of China (No. 51475255) for their financial support of this research.

6. References

- [1] Belhocine A, Bouchetara M, "Transient analysis of Thermoelastic contact problem of disk brakes," *Frontiers of Mechanical Engineering*, 2013. **8**(2): p. 150-159.
- [2] Majcherczak D, Dufrenoy P, Berthier Y, "Tribological, thermal and mechanical coupling aspects of the dry sliding contact," *Tribol Int.*, 2007. **40**: p. 834-43.
- [3] Simo JC, Miehe C, "Associative coupled thermoplasticity at finite strains: formulation, numerical analysis and implementation," *Comput Methods Appl Mech Eng.*, 1992. **98**: p. 41-104.
- [4] Heckmann A, "A brake model with Thermoelastic disc for the analysis of vehicle judder vibrations". *Vehicle system dynamics*, 2006. **44**: p. 360-367.
- [5] Podra P, Andersson S, "Simulating sliding wear with finite element method," *Tribology International*, 1999. **32**(2): p. 71-81.
- [6] Chantrenne P, Raynaud M, "A microscopic thermal model for dry sliding contact," *Int. J Heat Mass Transfer*, 1997. **40**: p. 1083-94.
- [7] Rezaei A, Van Paepegem W, De Baets P, "Adaptive finite element simulation of wear evolution in radial sliding bearings," *Wear*, 2012. **296**: p. 660-671.
- [8] Cai P, Wang Y, Wang T, Wang Q, "Effect of resins on thermal, mechanical and tribological properties of friction materials," *Tribol Int.*, 2015. **87**: p. 1-10.
- [9] Ireman P, Klarbring A, Stromberg N, "Finite element algorithms for Thermoelastic wear problems," *European Journal of Mechanics-A/Solids*, 2002. **21**(3): p. 423-440.
- [10] Wu L, Wen Z, Li W, Jin X, "Thermo-elastic-plastic finite element analysis of wheel/rail sliding contact. In: Proceedings of the 8th international conference on contact mechanics and wear of rail/wheel systems," *Florence, 2009*. **271**; 2011. p. 437-43.
- [11] Ostermeyer GP, Graf M, "Influence of wear on Thermoelastic instabilities in automotive brakes," *Wear*, 2013. **308**(1): p. 113-120.
- [12] Liangjin Gui, Xiaoying Wang, Zijie Fan, Fangyu Zhang, "A simulation method of thermo-mechanical and tribological coupled analysis in dry sliding system," *Tribology International*, 2016. **103**: p. 121-131.
- [13] Mazahery A, Shabani MO, "The accuracy of various training algorithms in tribological behaviour modelling of A356-B4 Composites," *Russ Metall*, 2011. **46**(21): p. 699-707.
- [14] Zienkiewicz OC, Taylor RL, Zienkiewicz OC, Taylor RL, "The finite element method," *London: McGraw-hill*, 1977.
- [15] *Abaqus Analysis User's Manual*, §6.5.2 Uncoupled heat transfer analysis. Adaptive manual version **6.12-1**, Dassault Systems Simulia Corp., Providence, RI; 2012.
- [16] Huang H-C, Usmani AS, "Finite element analysis for heat transfer," *London: Springer*, 1994.
- [17] *Abaqus Analysis User's Manual*, §12.2ALE. Adaptive manual version **6.12-1**, Dassault Systems Simulia Corp., Providence, RI; 2012.

- [18] Soderberg A, Andersson S, “Simulation of wear and contact pressure distribution at the pad-to-rotor interface in a disc brake using general purpose finite element analysis software”. *Wear*, 2009. **267**: p. 2243-51.